NASA TECHNICAL NOTE

NASA TN D-5769

SIMULATION IN GROUND-TEST FACILITIES OF ABLATION PERFORMANCE OF CHARRING ABLATORS DURING ATMOSPHERIC ENTRY

by Stephen S. Tompkins

Langley Research Center
Langley Station, Hampton, Va.

NATIONAL AERONAUTICS AND SPACE ADMINISTRATION • WASHINGTON, D. C. • APRIL 1970

1. Report No.	2. Government Accession No.	3. Recipient's Catalog No.
NASA TN D-5769		

4. Title and Subtitle	5. Report Date
SIMULATION IN GROUND-TEST FACILITIES OF ABLATION PERFORMANCE OF CHARRING ABLATORS DURING ATMOSPHERIC ENTRY	April 1970
	6. Performing Organization Code

7. Author(s)	8. Performing Organization Report No.
Stephen S. Tompkins	L-6516
	10. Work Unit No.
9. Performing Organization Name and Address	124-07-13-01-23
NASA Langley Research Center Hampton, Va. 23365	11. Contract or Grant No.
	13. Type of Report and Period Covered
12. Sponsoring Agency Name and Address	Technical Note
National Aeronautics and Space Administration Washington, D.C. 20546	14. Sponsoring Agency Code

15. Supplementary Notes

Some of the material in this paper was included in a thesis entitled "A Study of the Simulation of the Flight Performance of Charring Ablators in Ground Facilities" submitted in partial fulfillment of the requirements for the degree of Master of Aerospace Engineering, University of Virginia, Charlottesville, Virginia, June 1968.

16. Abstract

An analytical and experimental investigation is presented to establish a technique by which the performance of charring ablators in high-enthalpy environments can be simulated in low-enthalpy environments. Relationships are presented which indicate that proper simulation can be achieved by adjusting the heat input and stream oxygen content in the low-enthalpy environment. The technique is subject to the assumption that diffusion-controlled oxidation is the only mechanism of char removal.

Tests with two phenolic-nylon charring ablators were made at two enthalpy levels to validate the simulation technique. Nominal values of the principal test parameters for the two environments were as follows: For enthalpy, 10 000 and 3000 Btu/lbm (23 and 7 MJ/kg); for cold-wall convective heating rates, 155 and 145 Btu/ft^2-s (1.8 and 1.6 MW/m^2); and for stream oxygen mass fractions, 0.23 and 0.05. A comparison of the ablation performance data indicates that satisfactory simulation was obtained.

17. Key Words (Suggested by Author(s))	18. Distribution Statement
Ablation Thermal protection Heat shields	Unclassified – Unlimited

19. Security Classif. (of this report)	20. Security Classif. (of this page)	21. No. of Pages	22. Price*
Unclassified	Unclassified	36	$3.00

*For sale by the Clearinghouse for Federal Scientific and Technical Information
Springfield, Virginia 22151

SIMULATION IN GROUND-TEST FACILITIES OF ABLATION PERFORMANCE OF CHARRING ABLATORS DURING ATMOSPHERIC ENTRY*

By Stephen S. Tompkins
Langley Research Center

SUMMARY

An analytical and experimental investigation is presented to establish a technique by which the performance of charring ablators in atmospheric entry (high-enthalpy environment) can be simulated in ground-test facilities (low-enthalpy environment). Relationships are presented which indicate that proper simulation can be achieved by adjusting the heat input and stream oxygen content in the low-enthalpy environment. The technique is subject to the assumption that diffusion-controlled oxidation is the only mechanism of char removal.

Tests with two phenolic-nylon charring ablators were made at two enthalpy levels to validate the simulation technique. Nominal values of the principal test parameters for the two environments were as follows: For enthalpy, 10 000 and 3000 Btu/lbm (23 and 7 MJ/kg); for cold-wall convective heating rates, 155 and 145 Btu/ft^2-s (1.8 and 1.6 MW/m^2); and for stream oxygen mass fractions, 0.23 and 0.05. A comparison of the ablation performance data indicates that satisfactory simulation was obtained.

Although convective heating at constant enthalpy was the only case considered in the tests, a method to extend the present technique to obtain simulation with radiation as the prime source of heat is outlined in an appendix.

INTRODUCTION

Experimental studies of ablation materials are conducted in a variety of test facilities which produce a wide range of environments. These environments often provide

*Some of the material in this paper was included in a thesis entitled "A Study of the Simulation of the Flight Performance of Charring Ablators in Ground Facilities" submitted in partial fulfillment of the requirements for the degree of Master of Aerospace Engineering, University of Virginia, Charlottesville, Virginia, June 1968.

heating rates associated with atmospheric entry, but are usually characterized by low-enthalpy levels. The available high-enthalpy environment facilities are usually restricted to tests of small specimens and are therefore useful only for materials evaluation tests. Some low-enthalpy environments can be used to test much larger specimens, and combined thermal and mechanical behavior can be investigated. However, at low-enthalpy levels, ablation performance (i.e., surface recession, char thickness, and internal-temperature histories) differs from that at high-enthalpy levels unless appropriate test parameters are properly related.

Reference 1 provides a convenient approximate ablation analysis to examine the conditions under which the ablation performance of a charring ablator in a high-enthalpy environment, typical of reentry, can be simulated (reproduced) in a low-enthalpy test facility. This analysis is subject to the assumption that diffusion-controlled oxidation is the only mechanism of char removal. Reference 2 presents equations, derived from reference 1, that relate two environments in which the same ablation performance can be obtained. However, these equations lack sufficient detail for general experimental implementation. The present paper reviews the technique in reference 2 and extends the theory to provide the detail necessary for general experimental implementation.

Limited test data are also given in reference 2 which indicate that the same overall performance was obtained in two different but related environments. These data are for one charring ablation material and indicate that surface recession and final char thickness can be duplicated. In the present study, the complete reproduction of the transient ablation performance of two ablation materials is considered, as well as the net recession and final char thickness. Experimental results for a low-density and a high-density charring ablator are presented to evaluate the simulation that can be achieved. Surface recession, char thickness, and internal-temperature histories are compared to make this evaluation.

In an appendix, an extension of the analysis in reference 1 is presented to include the case in which convective heating is supplemented or replaced by radiant heating.

SYMBOLS

The units used for the physical quantities are given both in the U.S. Customary Units and in the International System of Units (SI). Factors relating the two systems are given in reference 3, and those used in the present investigation are presented in appendix A.

$a = \lambda C_e$

C oxygen concentration by mass

f	volatile fraction of uncharred material
H	total enthalpy
Δh	heat of combustion per unit mass of char consumed
Δh_{eff}	effective heat of pyrolysis
k	thermal conductivity
$\dot{m}(O_2)$	mass flux of oxygen
$\dot{m}_c$	rate of char loss
$\dot{m}_p$	rate of pyrolysis
$\vec{n}$	vector normal to surface
p	pressure
Q_c	integrated hot-wall convective heat input to nonablating surface
$q_{c,C}$	cold-wall convective heating rate with no ablation
$q_{c,net}$	net convective heating rate (see eq. (1))
$q_{c,H}$	hot-wall convective heating rate with no ablation
q_r	radiant heating rate
R_b	cylindrical body radius
S	distance from stagnation point along surface
T	temperature
t	time

$\vec{t}$	vector tangent to surface
W_c	char mass
$W_{c,i}$	initial char mass
α	absorptance of char
β	thermal transport parameter (see eq. (7))
γ	heat-transfer coefficient (see eq. (B2))
ϵ	emittance
η	transpiration coefficient
λ	mass of char removed per unit mass of oxygen
ρ	char density
σ	Stefan-Boltzmann constant
τ	shear stress

$$\phi = 1 + \frac{\eta\left(a\ \Delta h + H_e - H_w\right)}{\Delta h_{eff}(1 + a\eta)}$$

$$\psi = 1 + \frac{a\eta\ \Delta h}{\Delta h_{eff}(1 + a\eta)}$$

Subscripts:

e	external to boundary layer
m	extremum
p	pyrolysis
r	reference

s	stagnation point
w	wall
1	high-enthalpy environment
2	low-enthalpy environment

ANALYSIS

Basic Considerations

Simulation of ablator performance has been examined in references 1, 2, and 4. This section reviews the technique presented in reference 2 and extends the theory to provide the detail necessary for experimental implementation.

Aerodynamic inputs to an ablator may be broadly classified as thermal, chemical, and mechanical. The governing equations show that these inputs directly affect ablation performance only at the ablating surface. Therefore, any two environments which produce the same values of these inputs at the surface must yield identical ablation performance when applied to identical test specimens.

The aerodynamic inputs can be represented as follows:

Thermal	$\alpha q_r + q_{c,net}$
Chemical	$\dot{m}(O_2)$
Mechanical	$p_w\vec{n} + \tau_w\vec{t}$

The effects of mechanical inputs (shear stress and pressure) on char removal and mass transfer are neglected in the present study. However, in other applications, even at low shear stress, conditions may make it necessary to consider the effect of pressure. (See ref. 5.)

The thermal input is the radiant heating, after deducting reflection by the surface, plus convective heating corrected for surface temperature and mass transfer effects. The chemical input is primarily oxygen, which reacts with the char surface. The only char-surface removal mechanism considered in this study is diffusion-controlled oxidation, which depends on the oxygen flux across the boundary layer. However, surface mass transfer strongly influences this oxygen flux. Other boundary-layer species may react with the surface, but since the same considerations apply as for oxygen, these species will not be treated in the present paper.

Surface mass transfer can significantly reduce both heat and oxygen flux at the surface, and the magnitude of this reduction depends greatly on the stream enthalpy. However, the surface mass transfer is unknown because the instantaneous heat and oxygen fluxes are also unknown. Resolution of this problem is the key to producing in one environment the same ablation performance as that obtained in a different environment.

It should be noted that the relationship between surface mass transfer and heat and oxygen fluxes is known; that is, given the mass transfer $(\dot{m}_c + \dot{m}_p)$ and the heating rate to a nonablating wall $q_{c,H}$, the heating rate to an ablating wall is

$$q_{c,net} = q_{c,H} - (\dot{m}_c + \dot{m}_p)\eta(H_e - H_w) \tag{1}$$

Furthermore, for a Lewis number of unity and diffusion-controlled oxidation, the oxygen flux across the boundary layer is (ref. 1)

$$\dot{m}(O_2) = \frac{q_{c,net}}{H_e - H_w} C_e \tag{2}$$

The ideas developed to this point are adequate to permit the experimental reproduction in one environment of the ablation performance in a different environment without further theoretical development. However, such a solution would require an iterative and tedious test procedure. It might be argued that since the governing mechanisms have been assumed in this development, the ablation performance can be calculated directly and thereby eliminate much tedious testing. However, several reasons for not calculating the ablation performance can be cited. First, it may be desirable to examine interactions between heat shields and other systems at full scale so that ablation performance is not the only factor under consideration. Second, no ablation analysis can be conducted with as few assumptions as required for the tests. Therefore, the test results should be more accurate than calculations. Finally, analysis can be used to greatly reduce the number of tests required. The following section utilizes the approximate ablation analysis of reference 1 to quantitatively relate two environments so that the same ablation performance can be obtained in each.

Simulation Relationships

To simulate high-enthalpy ablation performance under given heat-transfer and energy conditions in a different environment, good estimates of mass transfer and surface temperature at high enthalpy must be available. Reradiation from the surface largely controls surface temperature; therefore, the temperature can be calculated from

$$T_w \approx \left(\frac{q_{c,C}}{\sigma\epsilon}\right)^{1/4}$$

This equation is adequate for determining surface temperature unless $q_{c,C}$ is very strongly influenced by the ablative process.

Evaluation of the surface mass transfer is much more complex. Both surface oxidation and internal pyrolysis contribute to the mass flux. The relative magnitudes of these fluxes depend primarily on the char thickness. Reference 1 shows that for given environmental conditions there exists an extremum char thickness which is the steady-state char thickness for a given heating rate. Transient ablation performance depends primarily on the relative magnitude of the actual char thickness and its extremum value. Therefore, if one environment reproduces the transient ablation performance produced by a second environment, then the extremum char thickness in the two environments must be equal. When these extremum char thicknesses are equated, the following relation results (ref. 6):

$$\left(\frac{C_e}{H_e - H_w}\right)_2 = \frac{\left(\frac{C_e}{H_e - H_w}\right)_1}{\left[1 + \frac{\alpha q_r}{q_{c,H}}\left(\frac{1 - f + a\eta}{1 - f}\right)\right]_1} \tag{3}$$

where

$$a = \lambda C_e \tag{4}$$

Equation (3) relates oxygen concentration and stream enthalpy in the two environments by assuming diffusion-controlled oxidation and that radiant heating occurs only in environment 1. It can be seen immediately from equation (2) that with no radiant heating and equal net convective heating, environments related by equation (3) will produce the same oxygen flux to the surface.

Now that the stream oxygen concentrations in the two environments have been related (eq. (3)), a relationship between the heat inputs in the two environments is needed. The heat inputs can be related by considering the approximate relation between the mass of char accumulated during a time interval of constant enthalpy and the heat input to a nonablating surface, equation (20a) in reference 1,

$$\frac{aQ_c}{(1 + a\eta)(H_e - H_w)W_{c,m}} = \frac{W_{c,i} - W_c}{W_{c,m}} - \left(1 + \frac{\phi\beta}{W_{c,m}}\right) \log_e \left(\frac{1 - \frac{W_c}{W_{c,m}}}{1 - \frac{W_{c,i}}{W_{c,m}}} \right) \tag{5}$$

where

$$\phi = 1 + \frac{\eta(a\,\Delta h + H_e - H_w)}{\Delta h_{eff}(1 + a\eta)} \tag{6}$$

and

$$\beta = \frac{k_r \rho}{\sigma\epsilon(T_r^2 + T_p^2)(T_r + T_p)} \tag{7}$$

As noted, equation (5) applies only for constant-enthalpy heating. However, the present approach can be extended to simulations in which enthalpy varies in one or both environments. All that is required is that the heating pulse be divided into a series of steps, each of which is treated as having a constant enthalpy equal to the average value during the step.

If the two environments produce the same ablation performance, the masses of char accumulated are necessarily equal at corresponding times. If the right-hand side of equation (5) is defined as $F(\phi,\beta,W_c,W_{c,i},W_{c,m})$, then equation (5) takes the following forms:

For environment 1,

$$\left[\frac{aQ_c}{(1 + a\eta)(H_e - H_w)}\right]_1 = F(\phi_1,\beta,W_c,W_{c,i},W_{c,m}) \tag{8}$$

and, for environment 2,

$$\left[\frac{aQ_c}{(1 + a\eta)(H_e - H_w)}\right]_2 = F(\phi_2,\beta,W_c,W_{c,i},W_{c,m}) \tag{9}$$

These equations relate the integrated heat input to a nonablating surface in the two environments through the parameter W_c. Furthermore, since the heat-transfer rate is assumed known in the environment that is to be simulated, the integrated heat input, and hence W_c, can be related to time. Therefore, the heating history that is required to

achieve transient simulation can easily be determined with the use of equations (3), (8), and (9).

An experimental evaluation of the preceding simulation technique has been made by using only convective heating at constant enthalpy in both environments. Stream oxygen concentration and heat input required for simulation were obtained with equations (3), (8), and (9). This evaluation will be discussed in the remaining sections of this paper. Although the tests show the application of the present technique at an enthalpy difference of about 6000 Btu/lbm (14 MJ/kg), this technique can be used for any enthalpy difference where surface recession results only from diffusion-controlled oxidation. An extension of the present technique to environments in which radiant heating is used in the simulation is discussed in appendix B.

TEST SPECIMENS

Materials

Two char-forming ablation materials were used in this investigation. One material contained 50 percent, by mass, powdered nylon and 50 percent powdered phenolic resin and was pressure-molded to a density of 75 lbm/ft^3 (1200 kg/m^3). The other material contained 40 percent powdered nylon, 37 percent powdered phenolic resin, and 23 percent phenolic microspheres and was pressure-molded to a density of 34 lbm/ft^3 (545 kg/m^3). The thermophysical properties used in the present analysis are given in table I. These materials represent two types of ablation materials that have been extensively tested. The low-density material is representative of a group of materials that has been flight-tested and may have application to future spacecraft.

Geometry and Construction

The test specimens were 2.5-inch-diameter (6.4-cm) cylinders, 1.25 inches (3.2 cm) thick, with a 4.7-inch-radius (11.9-cm) spherical face, machined from large blanks of the phenolic-nylon materials. The specimen geometry was designed to provide uniform heating and pressure across most of the surface. These cylinders were bonded to bakelite holders. (See fig. 1.)

There were eight specimens of each material, three of which contained 1-inch-diameter (2.54-cm) instrumented plugs. (See fig. 2.) Each plug contained four No. 36 gage chromel-alumel thermocouples installed in accordance with reference 7. The thermocouple junctions were located nominally at 0.125, 0.25, 0.375, and 0.5 inch (0.32, 0.64, 0.95, and 1.27 cm) from the front surface. The actual thermocouple-junction locations were determined with X-rays and are noted on the corresponding temperature histories.

APPARATUS AND TESTS

Apparatus

All ablation specimens were tested in supersonic arc-powered tunnels at the Langley Research Center. The low-enthalpy tests were conducted in a 5-megawatt ac arc-powered tunnel at the apparatus B of the Langley entry structures facility. A conical nozzle with a throat diameter of 1.5 inches (3.8 cm) and an exit diameter of 4 inches (10 cm) was used. The desired stream oxygen concentrations were obtained by mixing air and nitrogen.

The high-enthalpy tests were conducted in a 1-megawatt dc arc-powered tunnel at the apparatus D of the Langley entry structures facility. A conical nozzle with a 1-inch-diameter (2.5-cm) throat and a 4-inch-diameter (10-cm) exit was used. The desired stream oxygen concentrations were obtained by mixing oxygen and nitrogen.

Tests

Nominal test conditions (table II) were determined as follows. The enthalpy level, heating rate, and oxygen concentration for environment 1 were chosen to insure a diffusion-controlled oxidation regime in all tests. Convective heating was the only mode of heat transfer present in these two environments. An enthalpy of 3000 Btu/lbm (7 MJ/kg) for environment 2 was selected, and the corresponding heat input and stream chemical composition required for simulation were determined by using equations (3), (8), (9), and the properties given in table I. The conditions required for simulation are dependent upon material properties. (See eqs. (3) and (5).) However, the required conditions associated with the two materials considered herein were essentially the same. The required conditions for the low-density material were C_e = 5 percent and $q_{c,C}$ = 150 Btu/ft^2-s $\left(1.7 \text{ MW/m}^2\right)$, and those for the high-density material were C_e = 5 percent and $q_{c,C}$ = 140 Btu/ft^2-s $\left(1.6 \text{ MW/m}^2\right)$. Hence, only one set of conditions for environment 2 is given in table II.

Tunnel operating conditions were measured for each test by means of pressure and heating-rate probes of the same size and shape as the specimens. The heating-rate probe was a thin-skin calorimeter. The pressure and heating-rate distributions over the specimen in the two environments are shown in figure 3. The same pressure and heating-rate distributions were obtained in the two environments. Heating-rate and pressure measurements were made prior to and after the specimen was exposed to the test stream. The measurements of pressure, heating rates, and stream oxygen concentrations were accurate within ±10 percent. Total enthalpy of the test streams was determined by using references 8, 9, 10, and the measured stagnation pressure and heating rate.

Specimens were tested for 30, 60, 90, and 120 seconds. The instrumented specimens used to evaluate transient ablation simulation were tested for 120 seconds. Each specimen tested at the high-enthalpy condition for a given time had a corresponding specimen tested at the prescribed low-enthalpy condition for the same length of time. All temperature and pressure data were recorded by the Langley central digital data recording facility. Thickness measurements were accurate within ±0.01 inch (±0.03 cm).

RESULTS AND DISCUSSION

Eight pairs of specimens were tested in low- and high-enthalpy environments related through equations (3), (8), and (9). Four pairs were made of the low-density material, indicated by an LD prefix to the specimen number, and four pairs were made of the high-density material, indicated by an HD prefix to the specimen number. The test data are summarized in table III.

Comparison of Measured and Required Test Conditions

Table II presents the nominal test conditions required for simulation. All tests for both environments were made prior to any data reduction, and the measured values of the parameters varied from the nominal values. (See table III.) The most substantial deviation from the nominal condition occurred at high enthalpy for specimens LD-5 and HD-7 because of an oxygen-rich stream which resulted from problems in the flow control system.

Table III also shows required heating rates and oxygen concentrations for simulation at the measured low enthalpies based on the measured conditions at high enthalpies. The agreement between the required and measured heating rates and oxygen concentration, in most cases, is not good. However, in the diffusion-controlled oxidation regime, the value of a single input $\left(\text{i.e., } q_{c,C} \text{ or } C_e\right)$ is not as important as the product of these inputs as long as the error in $q_{c,C}$ is small. (See eq. (2).) Although an error in $q_{c,C}$ will affect the surface temperature and ablation performance, the error is small due to the 1/4 power dependence of temperature on $q_{c,C}$. Therefore, if the product of $q_{c,C}$ and C_e (i.e., the oxygen mass flux to the surface) is correct, satisfactory reproduction of the surface recession, char thickness, and thickness of degraded material can be obtained as indicated by the test results.

The products of the required and measured values of $q_{c,C}$ and C_e are also presented in table III. Except for specimen LD-6, the products can be considered in satisfactory agreement when it is noted that the percent differences are within the accuracy of the measured data (i.e., about ±20 percent).

Low-Density Phenolic-Nylon Specimens

Photographs of the tested specimens are shown in figure 4. Total recession, char thickness, and thickness of degraded material for each specimen are given in table III and plotted in figure 5. Internal temperature histories for specimens LD-7 and LD-8 are shown in figure 6.

From a visual comparison of the paired specimens in figure 4, it is seen that the char surface and char structure are similar. The cracked pattern visible on the surface of each specimen is believed to have been formed during specimen cooling. Motion pictures taken during testing do not show this pattern in either environment.

An examination of the test data (surface recession and interface-location histories in fig. 5 and internal-temperature histories in fig. 6) shows that the transient ablation performance in a high-enthalpy environment of the low-density charring ablator was satisfactorily reproduced in a low-enthalpy test stream.

High-Density Phenolic-Nylon Specimens

Photographs of the tested specimens are shown in figure 7. The total recession, char thickness, and thickness of degraded material for each specimen are given in table III, and the data are plotted in figure 8. Internal-temperature histories for specimens HD-7 and HD-8 are shown in figure 9.

A visual comparison of the paired specimens in figure 7 shows that the char surface and structure are similar. As was previously mentioned, the cracked pattern present on all the char surface is believed to occur during cooling. The source of the sunburst pattern on the specimen tested for 30 seconds at low enthalpy is not known.

Figure 8 shows the histories of the pyrolysis zone and outer-surface location for the high-density phenolic-nylon specimens tested at the high- and low-enthalpy conditions. The agreement is good, and satisfactory reproduction of the transient surface and interface behavior is indicated.

Figure 9 shows internal-temperature histories for specimens tested at the low- and high-enthalpy conditions. The agreement is satisfactory. The differences may be attributed to the higher-than-required heating rate experienced by the specimen tested at low enthalpy. An examination of these test data shows that the transient ablation performance in a high-enthalpy environment of the high-density charring ablator was satisfactorily reproduced in a low-enthalpy test stream.

CONCLUDING REMARKS

The conditions under which the ablation and thermal performance of a charring ablator in a high-enthalpy environment can be simulated in a low-enthalpy environment have been examined. An approximate ablation analysis was used to obtain quantitative relationships between a constant low-enthalpy heating environment and a constant or variable high-enthalpy heating environment which produce the same ablation and thermal performance of a charring ablator. The analysis is subject to the assumption that diffusion-controlled oxidation is the only mechanism of char removal. Simulation with either convective and/or radiant heating was discussed.

Tests were made to determine the ablation performance of a low-density phenolic-nylon material and a high-density phenolic-nylon material in an oxygen-nitrogen gas mixture at a constant high-enthalpy convective heating condition. Identical specimens of each material were then tested in a constant low-enthalpy convective heating test stream properly related to the high-enthalpy environment. Satisfactory ablation performance simulation was obtained by proper adjustment of the stream composition and heat input in the low-enthalpy environment.

Langley Research Center,
National Aeronautics and Space Administration,
Langley Station, Hampton, Va., January 22, 1970.

APPENDIX A

CONVERSION OF U.S. CUSTOMARY UNITS TO SI UNITS

Conversion factors required for units used herein are given in the following table:

Physical quantity	U.S. Customary Units	Conversion factor (*)	SI units (**)
Density	lbm/ft^3	16.018463	kg/m^3
Enthalpy	Btu/lbm	2.324444×10^3	J/kg
Heating rate	$Btu/ft^2\text{-}s$	1.134893×10^4	W/m^2
Mass distribution	lbm/ft^2	4.882	kg/m^2
Temperature	^oR	5/9	K
Thermal conductivity . . .	$Btu/ft\text{-}s\text{-}^oR$	6.24×10^3	W/m-K
Thickness	in.	2.54×10^{-2}	m

*Multiply value given in U.S. Customary Unit by conversion factor to obtain equivalent value in SI unit.

**Prefixes to indicate multiples of units are as follows:

Prefix	Multiple
centi (c)	10^{-2}
kilo (k)	10^3
mega (M)	10^6

APPENDIX B

SIMULATION WITH RADIANT HEATING

Testing certain large heat-shield specimens may require more heat input to the material than a facility is capable of providing in the form of convective heating. In these cases, the convective heating can be supplemented or replaced with radiant heating, while the gas stream provides the appropriate chemical inputs to the surface. The remainder of this section presents the analysis required for simulation of ablation performance when radiant heating supplements convective heating.

When radiant heating and convective heating are present both in the ground-test facility and in the flight environment, the relationship between the stream oxygen concentrations (eq. (3)) becomes

$$\left(\frac{C_e}{H_e - H_w}\right)_2 = \left(\frac{C_e}{H_e - H_w}\right)_1 \frac{1 + \left(\frac{\alpha q_r}{q_{c,H}}\right)_2}{1 + \left(\frac{\alpha q_r}{q_{c,H}}\right)_1 \left(\frac{1 - f + a\eta}{1 - f}\right) - \left(\frac{\alpha q_r}{q_{c,H}}\right)_2 \frac{(H_e - H_w)_2 a_1 \eta}{(H_e - H_w)_1 (1 - f)}} \tag{B1}$$

The approximate analysis of reference 1 has been formulated so that radiant heating appears only in the ratio $\alpha q_r/q_{c,H}$. This term is assumed constant in the present analysis. Formulating the analysis in terms of the constant ratio $\alpha q_r/q_{c,H}$ eliminates the explicit appearance of the heat input due to radiation; only the convective heat input is specified. Therefore, only the required total convective heat input – hence the test time – is determined with equations (8) and (9) for given values of $q_{c,H}$ and $\alpha q_r/q_{c,H}$.

The equations from reference 1 require some alteration when radiant heating is the prime heating mode, that is, when it essentially replaces the convective heating mode. For this case, the gas flow over the surface is used only to provide the required oxidation of the surface and to remove the gaseous products of pyrolysis. The convective heating is approximately equal to zero; also, the difference between the enthalpy of the stream external to the boundary layer and that at the surface is zero. However, to obtain the correct mass flux of oxygen to the surface, the ratio of the heating rate to the enthalpy difference has a definite value, which is a heat-transfer coefficient:

$$\gamma = \frac{q_{c,net}}{H_e - H_w} \qquad \left(H_e \neq H_w\right) \tag{B2}$$

The extremum char mass then becomes (derived from ref. 1)

$$W_{c,m} = \beta\left[\frac{1 - f}{f}\left(\frac{\alpha q_r}{a\gamma\,\Delta h_{eff}} + \frac{\Delta h}{\Delta h_{eff}}\right) - 1\right] \tag{B3}$$

With this definition of $W_{c,m}$, the relationship between oxygen concentration and stream enthalpy in the two environments (eq. (3)) becomes

$$\frac{(C_e)_2}{(C_e)_1} = \frac{\left[\dfrac{\alpha q_r}{\gamma(H_e - H_w)}\right]_2}{\left[1 + \dfrac{\alpha q_r}{q_{c,H}}\left(1 + \dfrac{a\eta}{1 - f}\right)\right]} \tag{B4}$$

The approximate relation between the mass of char accumulated and the heat-transfer coefficient γ is

$$\frac{W_{c,i} - W_c}{W_{c,m}} - \left(1 + \frac{\psi\beta}{W_{c,m}}\right)\log_e\left(\frac{1 - \dfrac{W_c}{W_{c,m}}}{1 - \dfrac{W_{c,i}}{W_{c,m}}}\right) = \frac{a\gamma t}{(1 + a\eta)W_{c,m}} \tag{B5}$$

where

$$\psi = 1 + \frac{a\eta\,\Delta h}{\Delta h_{eff}(1 + a\eta)} \tag{B6}$$

Note that ψ and γt in equation (B5) are analogous to ϕ and Q_c in equation (5). Equation (B5) can be put in a form analogous to equation (9), that is,

$$\left(\frac{a\gamma t}{1 + a\eta}\right)_2 = F\left(\psi_2, \beta, W_c, W_{c,i}, W_{c,m}\right) \tag{B7}$$

Equations (8) and (B7) can now be used to relate the convective heat input $Q_{c,1}$ and the parameter $(\gamma t)_2$, respectively – both as a function of the parameter W_c. As stated previously, only the convective heat input – or test time – is specified rather than the total convective heat input plus radiant heat input.

REFERENCES

1. Swann, Robert T.: Approximate Analysis of the Performance of Char-Forming Ablators. NASA TR R-195, 1964.

2. Swann, Robert T. Dow, Marvin B.; and Tompkins, Stephen S.: Analysis of the Effects of Environmental Conditions on the Performance of Charring Ablators. J. Spacecraft Rockets, vol. 3, no. 1, Jan. 1966, pp. 61-67.

3. Comm. on Metric Pract.: ASTM Metric Practice Guide. NBS Handbook 102, U.S. Dep. Com., Mar. 10, 1967.

4. Tompkins, Stephen S.; and Dow, Marvin B.: Parametric Study of a Low-Density Charring Ablator. NASA TN D-3735, 1966.

5. Bush, Harold G.; and Dow, Marvin B.: Multidimensional Gas Flow Through Permeable Char Layers and Its Effect on Ablation. NASA TR R-296, 1969.

6. Tompkins, Stephen S.: A Study of the Simulation of the Flight Performance of Charring Ablators in Ground Facilities. M.A.E. Thesis, Univ. of Virginia, 1968.

7. Brewer, William D.: Effects of Thermocouple Wire Size and Configuration on Internal Temperature Measurements in a Charring Ablator. NASA TN D-3812, 1967.

8. Fay, J. A.; and Riddell, F. R.: Theory of Stagnation Point Heat Transfer in Dissociated Air. J. Aeronaut. Sci., vol. 25, no. 2, Feb. 1958, pp. 73-85, 121.

9. Hansen, C. Frederick: Approximations for the Thermodynamic and Transport Properties of High-Temperature Air. NASA TR R-50, 1959. (Supersedes NACA TN 4150.)

10. Zoby, Ernest V.; and Sullivan, Edward M.: Effects of Corner Radius on Stagnation-Point Velocity Gradients on Blunt Axisymmetric Bodies. NASA TM X-1067, 1965.

TABLE I.- MATERIAL PROPERTIES

	Low-density phenolic-nylon	High-density phenolic-nylon
Thermal transport parameter, β, lbm/ft^2 (kg/m^2)	0.115 (0.56)	0.19 (0.93)
Heat of combustion, Δh, Btu/lbm (MJ/kg)	5000 (11.62)	5000 (11.62)
Mass of char removed per unit mass of oxygen, λ	0.75	0.75
Volatile fraction of uncharred material, f	0.53	0.6
Effective heat of pyrolysis, Δh_{eff}, Btu/lbm (MJ/kg)	4340 (10.1)	4340 (10.1)
Transpiration coefficient, η	0.6	0.6
Emittance, ϵ	0.9	0.9
Reference thermal conductivity, k_r, Btu/ft-s-$^\circ$R (W/m-K)	3.61×10^{-4} (2.25)	3.19×10^{-4} (1.99)
Char density, ρ, lbm/ft^3 (kg/m^3)	16 (256)	30 (480)
Pyrolysis temperature, T_p, $^\circ$R (K)	1200 (667)	1200 (667)
Virgin material density, lbm/ft^3 (kg/m^3)	34 (545)	75 (1200)
Reference temperature, T_r, $^\circ$R (K)	4600 (2560)	4600 (2560)

TABLE II.- NOMINAL TEST CONDITIONS

	High enthalpy (Environment 1)	Low enthalpy (Environment 2)
Total enthalpy, Btu/lbm (MJ/kg)	10 000 (23)	3000 (7)
Free-stream Mach number	3	3
Specimen stagnation pressure, atm	0.04	0.37
Cold-wall stagnation heat-transfer rate, Btu/ft^2-s (MW/m^2)	155 (1.8)	145 (1.7)
Free-stream oxygen content, percent by mass	23	5
Specimen test time, s	Varied	Varied

TABLE III.- SUMMARY OF TEST DATA

(a) U.S. Customary Units

Specimen	$q_{c,C}$, Btu/ft^2-s		H_e, Btu/lbm	C_e, percent		Test time, s	Thickness change, in.	Char thickness, in.	Thickness of degraded material, in.	$q_{c,C}C_e$, Btu/ft^2-s	
	Required	Measured		Required	Measured					Required	Measured
LD-1		173	11 000		24	30	0.04	0.13	0.17		
LD-2	145	162	3 500	5.8	5.8	30	.03	.14	.17	8.4	9.2
LD-3		180	12 000		24	60	0.11	0.2	0.31		
LD-4	158	157	3 400	5.1	5.8	60	.11	.2	.31	8.1	9.1
LD-5		172	10 000		32	90	0.19	0.22	0.41		
[a]LD-6	163	164	3 500	8.6	5.8	90	.19	.23	.42	14	9.5
[a]LD-7		175	13 000		23	120	0.29	0.23	0.52		
[a]LD-8	170	164	3 500	4.6	5.8	120	.28	.21	.49	7.8	9.5
HD-1		161	9 000		24	30	0.01	0.07	0.08		
HD-2	138	159	3 600	7.6	5.8	30	.02	.08	.10	11	9.2
HD-3		160	9 000		24	60	0.05	0.12	0.17		
HD-4	144	165	3 500	7.3	5.5	60	.06	.12	.18	11	9.1
HD-5		160	10 000		26	90	0.07	0.16	0.23		
HD-6	145	160	3 600	7.3	5.8	90	.08	.17	.25	11	9.3
[a]HD-7		172	11 000		31	130	0.15	0.19	0.33		
[a]HD-8	150	167	3 500	7.5	5.8	121	.14	.2	.35	11	9.7

(b) SI Units

Specimen	$q_{c,C}$, MW/m^2		H_e, MJ/kg	C_e, percent		Test time, s	Thickness change, cm	Char thickness, cm	Thickness of degraded material, cm	$q_{c,C}C_e$, kW/m^2	
	Required	Measured		Required	Measured					Required	Measured
LD-1		1.96	25.60		24	30	0.102	0.330	0.432		
LD-2	1.65	1.84	8.14	5.8	5.8	30	.076	.356	.432	95	104
LD-3		2.04	27.89		24	60	0.280	0.508	0.787		
LD-4	1.79	1.78	7.90	5.1	5.8	60	.280	.508	.787	92	103
LD-5		1.95	23.24		32	90	0.483	0.559	1.04		
[a]LD-6	1.85	1.86	8.14	8.6	5.8	90	.483	.584	1.07	159	108
[a]LD-7		1.99	30.22		23	120	0.737	0.584	1.32		
[a]LD-8	1.93	1.86	8.14	4.6	5.8	120	.711	.533	1.24	89	108
HD-1		1.83	20.92		24	30	0.025	0.178	0.203		
HD-2	1.57	1.80	8.37	7.6	5.8	30	.051	.203	.250	125	104
HD-3		1.82	20.95		24	60	0.127	0.305	0.432		
HD-4	1.63	1.87	8.14	7.3	5.5	60	.152	.305	.457	125	103
HD-5		1.82	23.24		26	90	0.178	0.406	0.584		
HD-6	1.65	1.82	8.37	7.3	5.8	90	.203	.432	.635	125	105
[a]HD-7		1.95	25.60		31	130	0.381	0.483	0.838		
[a]HD-8	1.70	1.90	8.14	7.5	5.8	121	.356	.508	.889	125	110

[a]Instrumented specimens.

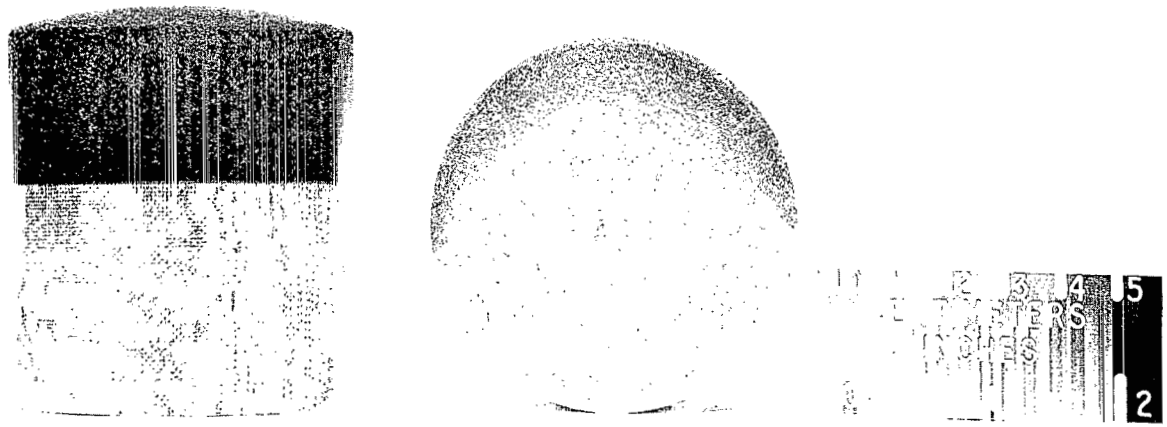

Uninstrumented specimen

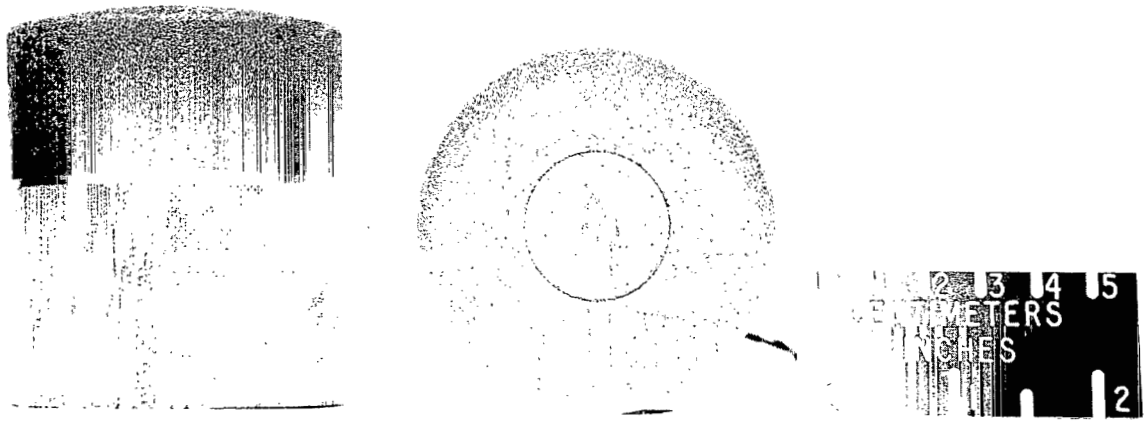

Instrumented specimen

(a) Low-density phenolic-nylon.

Figure 1.- Typical specimens before testing.

L-70-1527

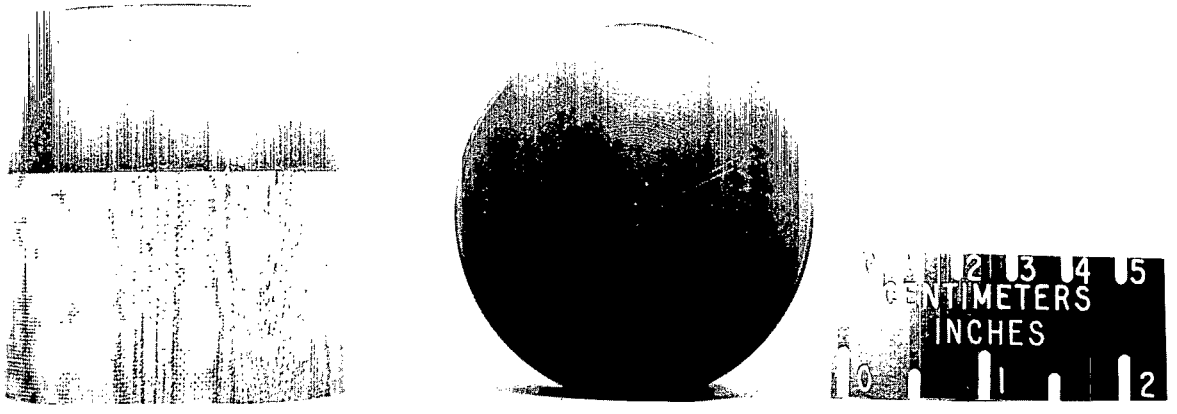

Uninstrumented specimen

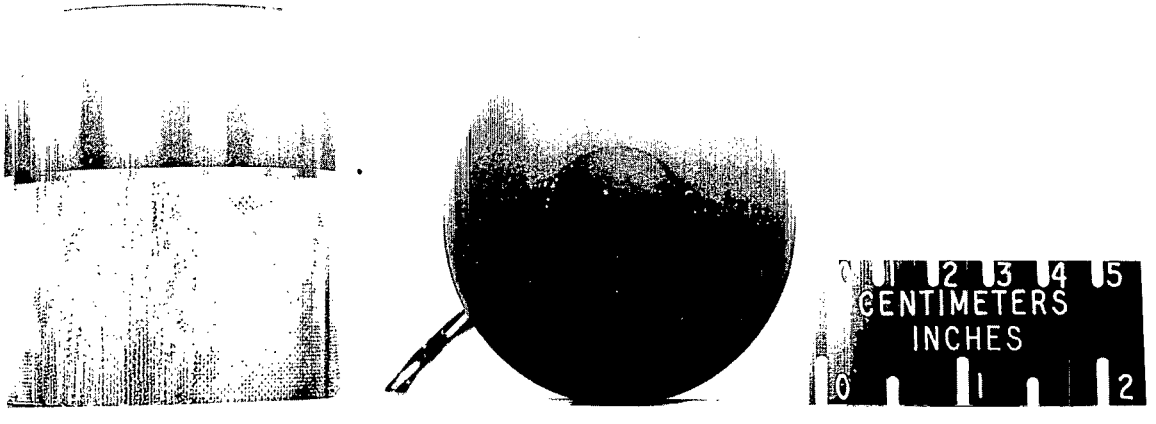

Instrumented specimen

(b) High-density phenolic-nylon.

Figure 1.- Concluded.

L-70-1528

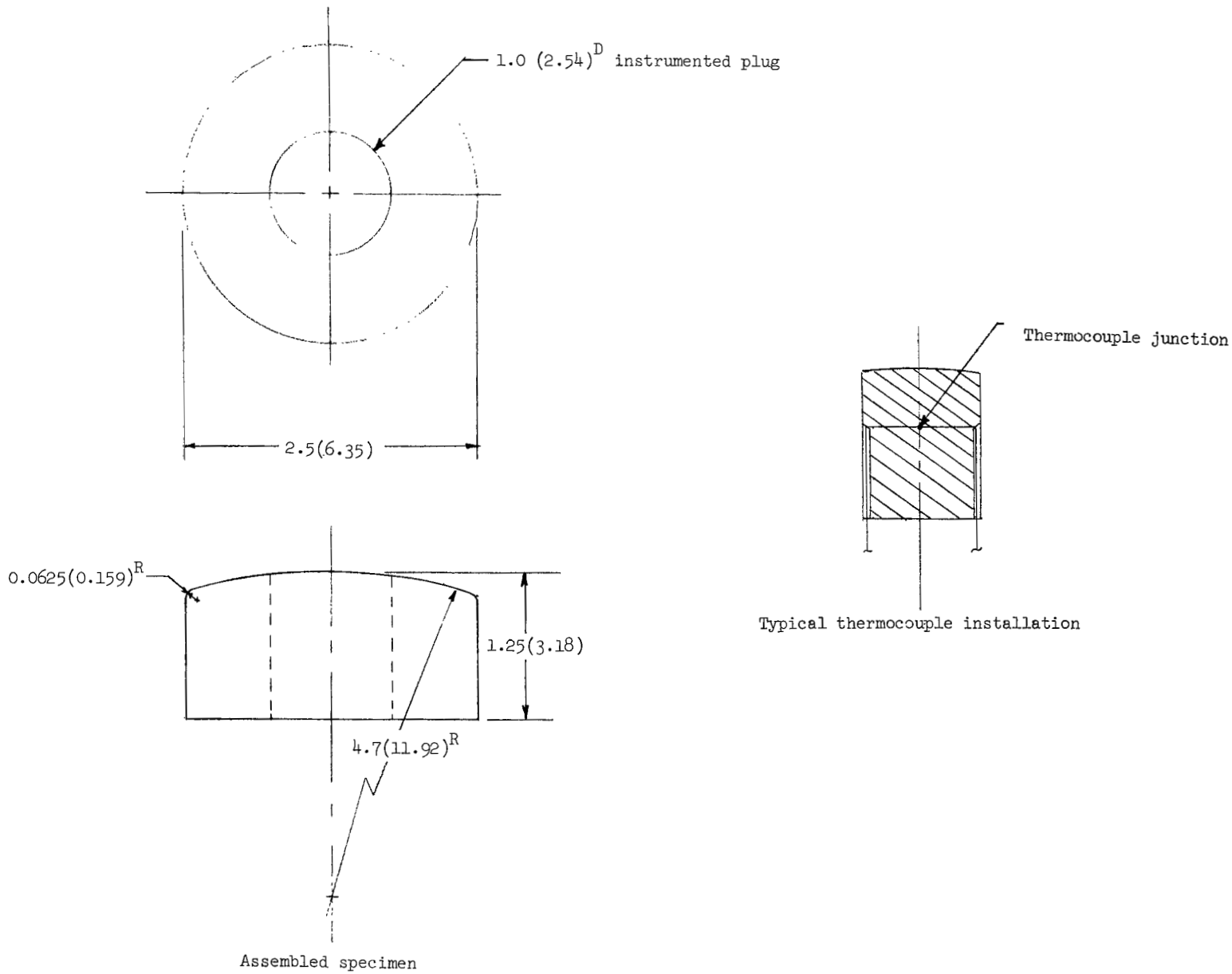

Figure 2.- Schematic diagram of typical instrumented specimen. All dimensions are given in inches (centimeters).

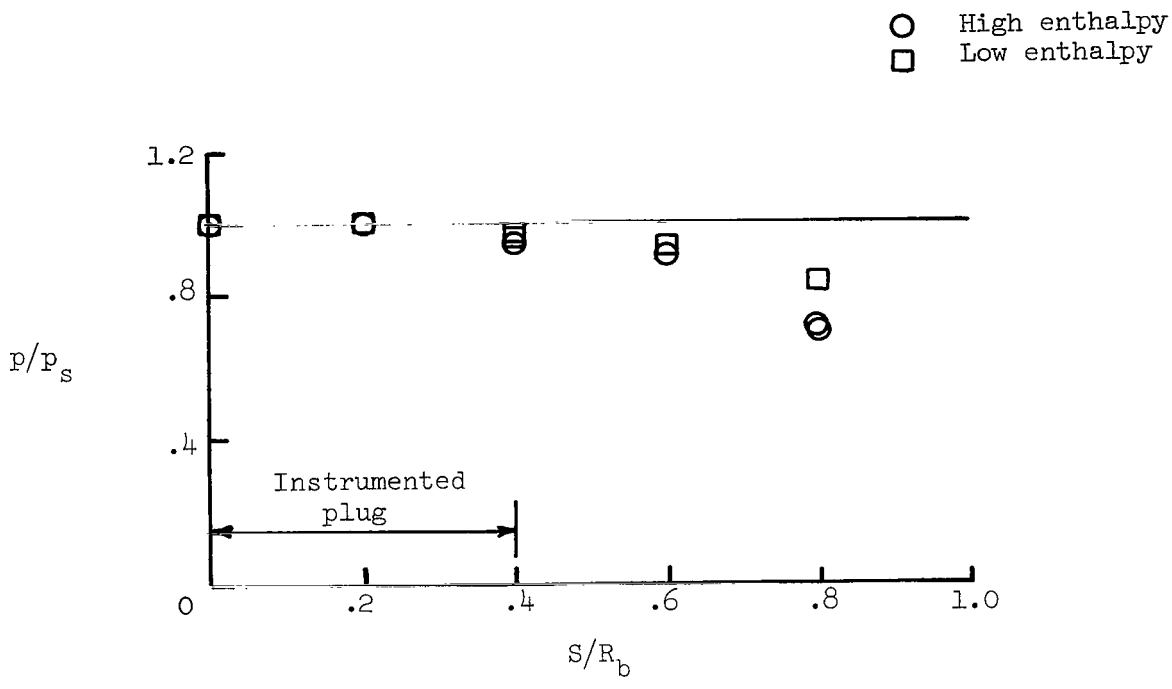

(a) Pressure distribution.

Figure 3.- Pressure and cold-wall heating-rate distributions.

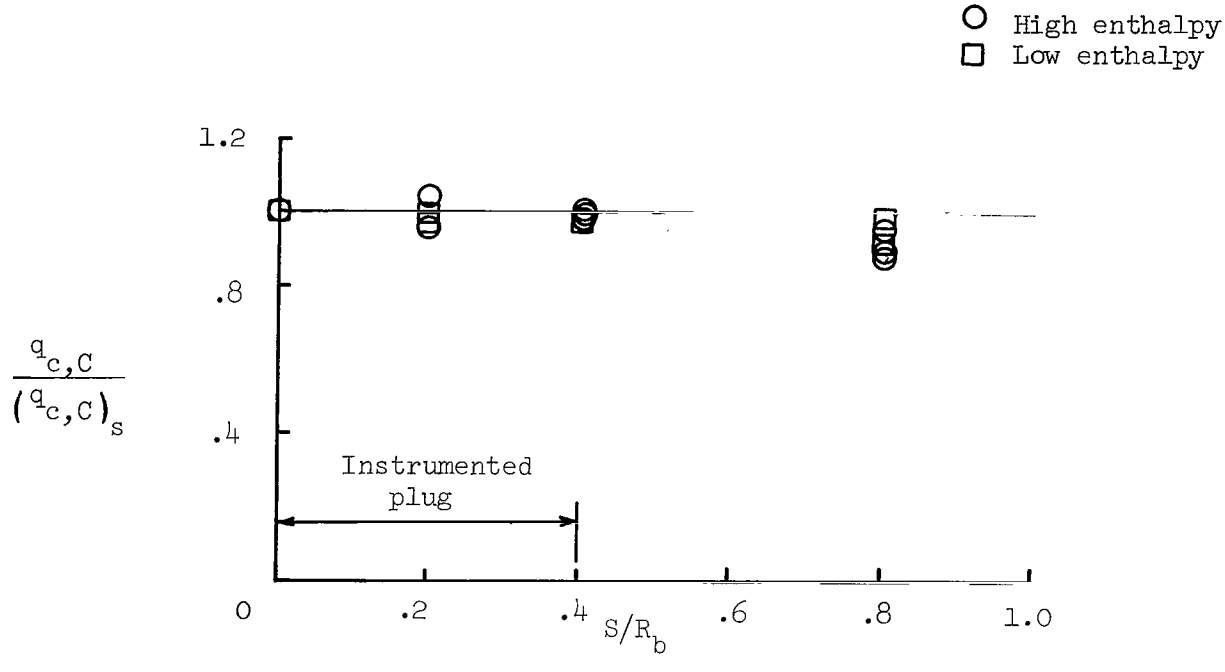

(b) Heating-rate distribution.

Figure 3.- Concluded.

(a) Specimen LD-1 tested 30 seconds at high enthalpy.

(b) Specimen LD-2 tested 30 seconds at low enthalpy.

Figure 4.- Low-density phenolic-nylon after testing. L-70-1529

(c) Specimen LD-3 tested 60 seconds at high enthalpy.

(d) Specimen LD-4 tested 60 seconds at low enthalpy.

Figure 4.- Continued.

L-70-1530

(e) Specimen LD-5 tested 90 seconds at high enthalpy.

(f) Specimen LD-6 tested 90 seconds at low enthalpy.

Figure 4.- Continued.

L-70-1531

(g) Specimen LD-7 tested 120 seconds at high enthalpy.

(h) Specimen LD-8 tested 120 seconds at low enthalpy.

Figure 4.- Concluded. L-70-1532

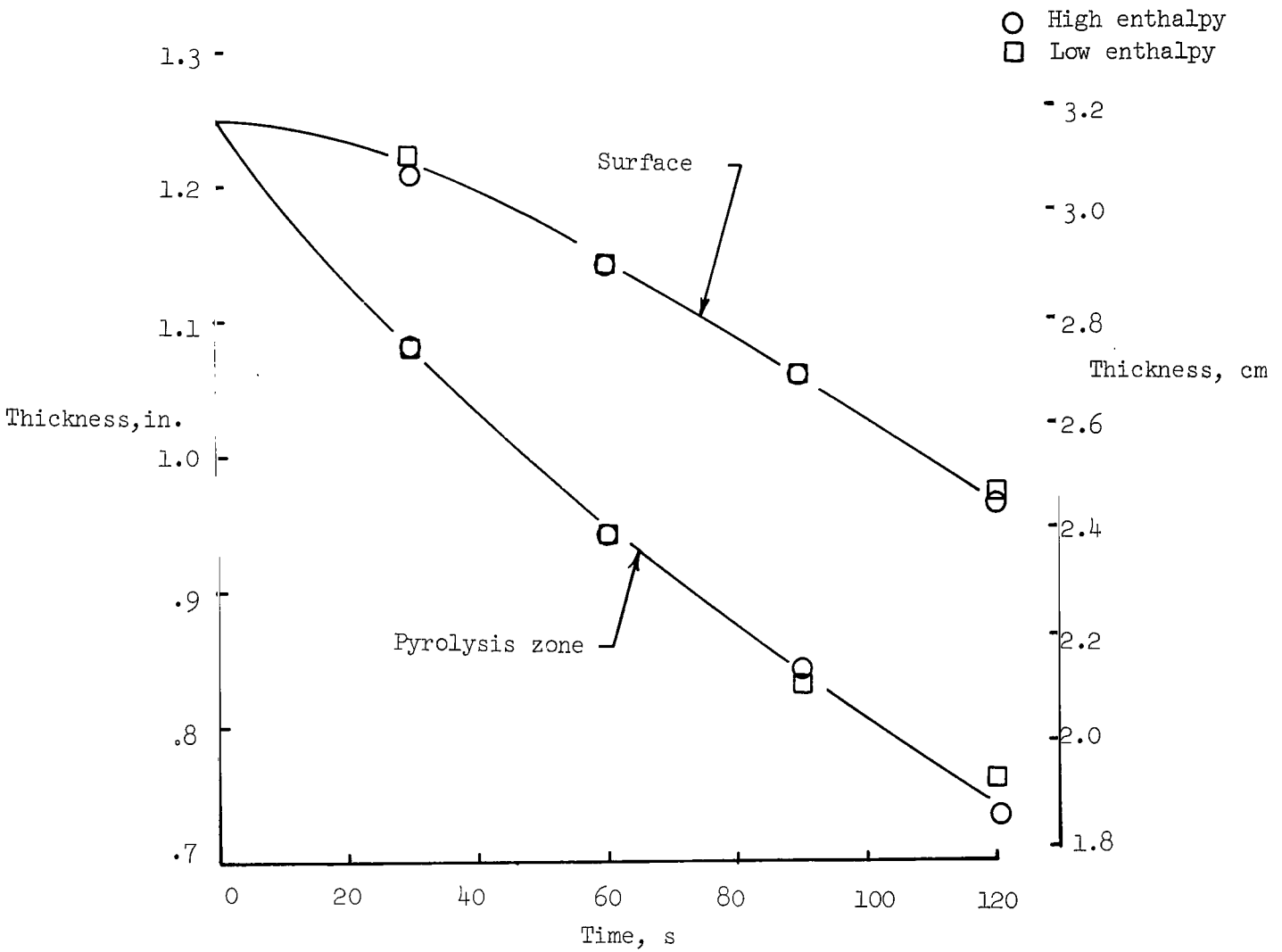

Figure 5.- Measured surface and interface-location histories for low-density phenolic-nylon specimens.

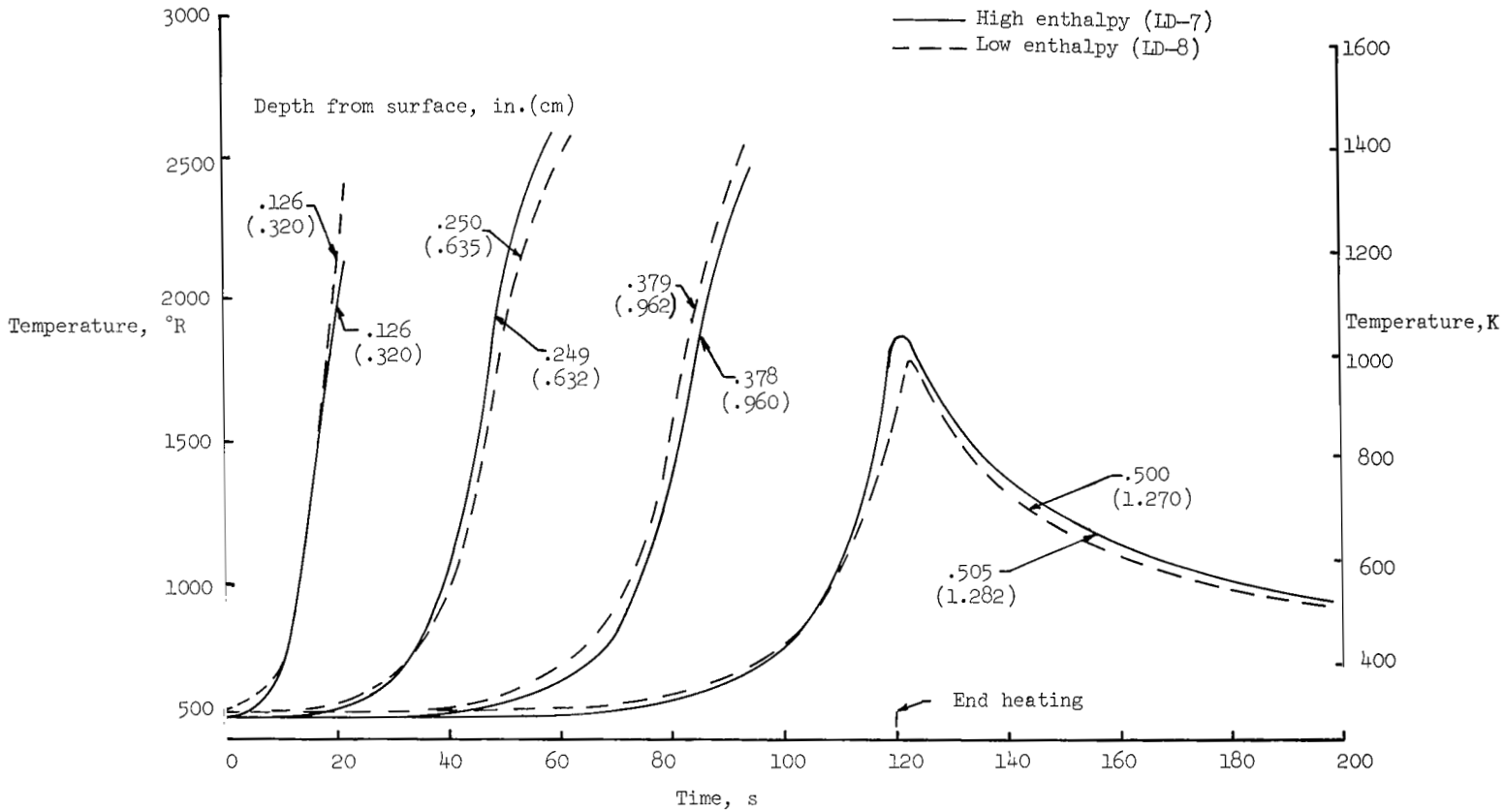

Figure 6.- Measured internal-temperature histories for two low-density phenolic-nylon specimens.

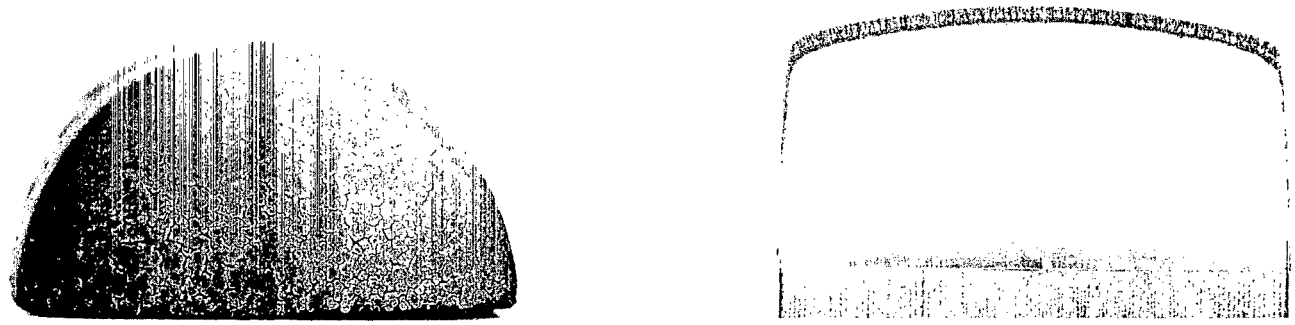

(a) Specimen HD-1 tested 30 seconds at high enthalpy.

(b) Specimen HD-2 tested 30 seconds at low enthalpy.

Figure 7.- High-density phenolic-nylon after testing. L-70-1533

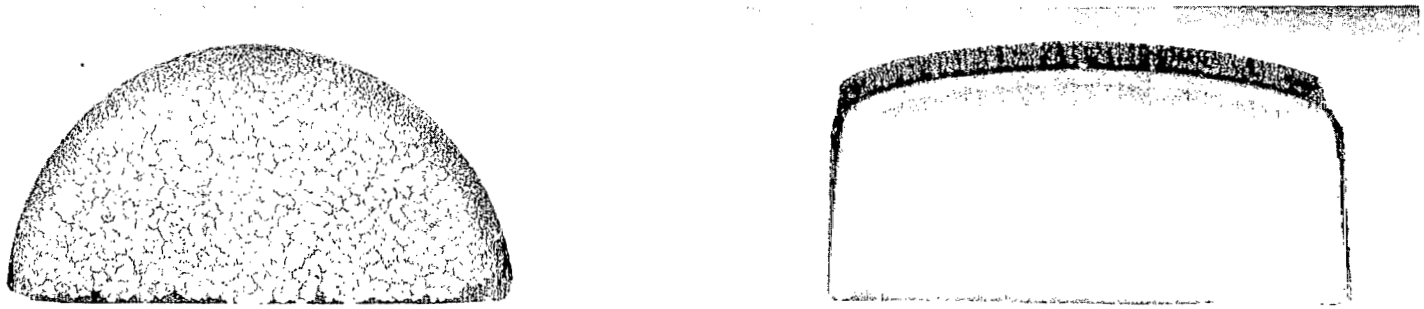

(c) Specimen HD-3 tested 60 seconds at high enthalpy.

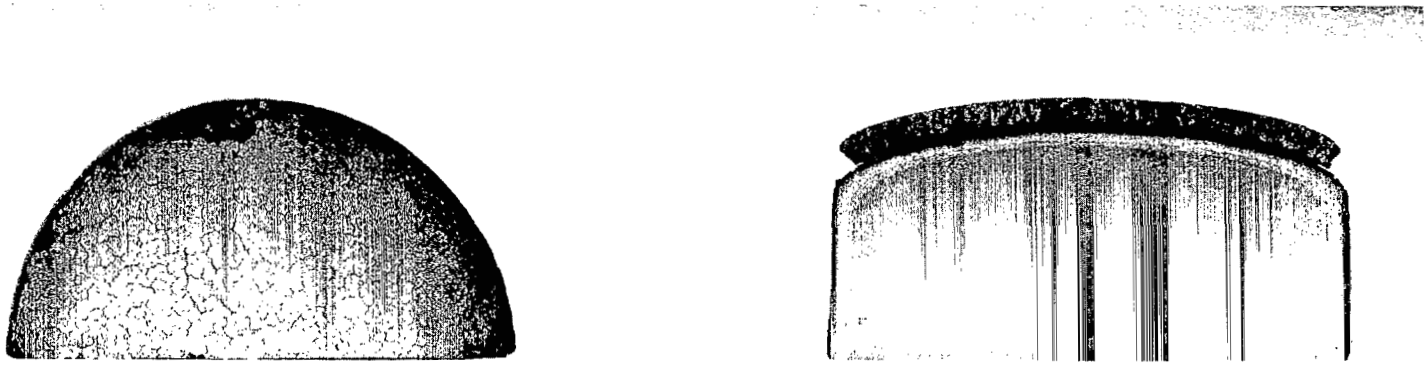

(d) Specimen HD-4 tested 60 seconds at low enthalpy.

Figure 7.- Continued.

L-70-1534

(e) Specimen HD-5 tested 90 seconds at high enthalpy.

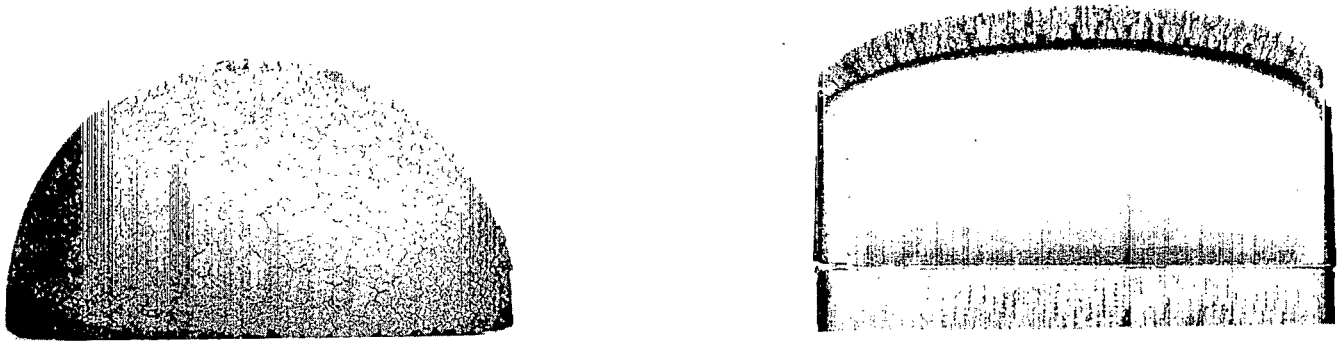

(f) Specimen HD-6 tested 90 seconds at low enthalpy.

Figure 7.- Continued.

L-70-1535

(g) Specimen HD-7 tested 130 seconds at high enthalpy.

(h) Specimen HD-8 tested 120 seconds at low enthalpy.

Figure 7.- Concluded.

L-70-1536

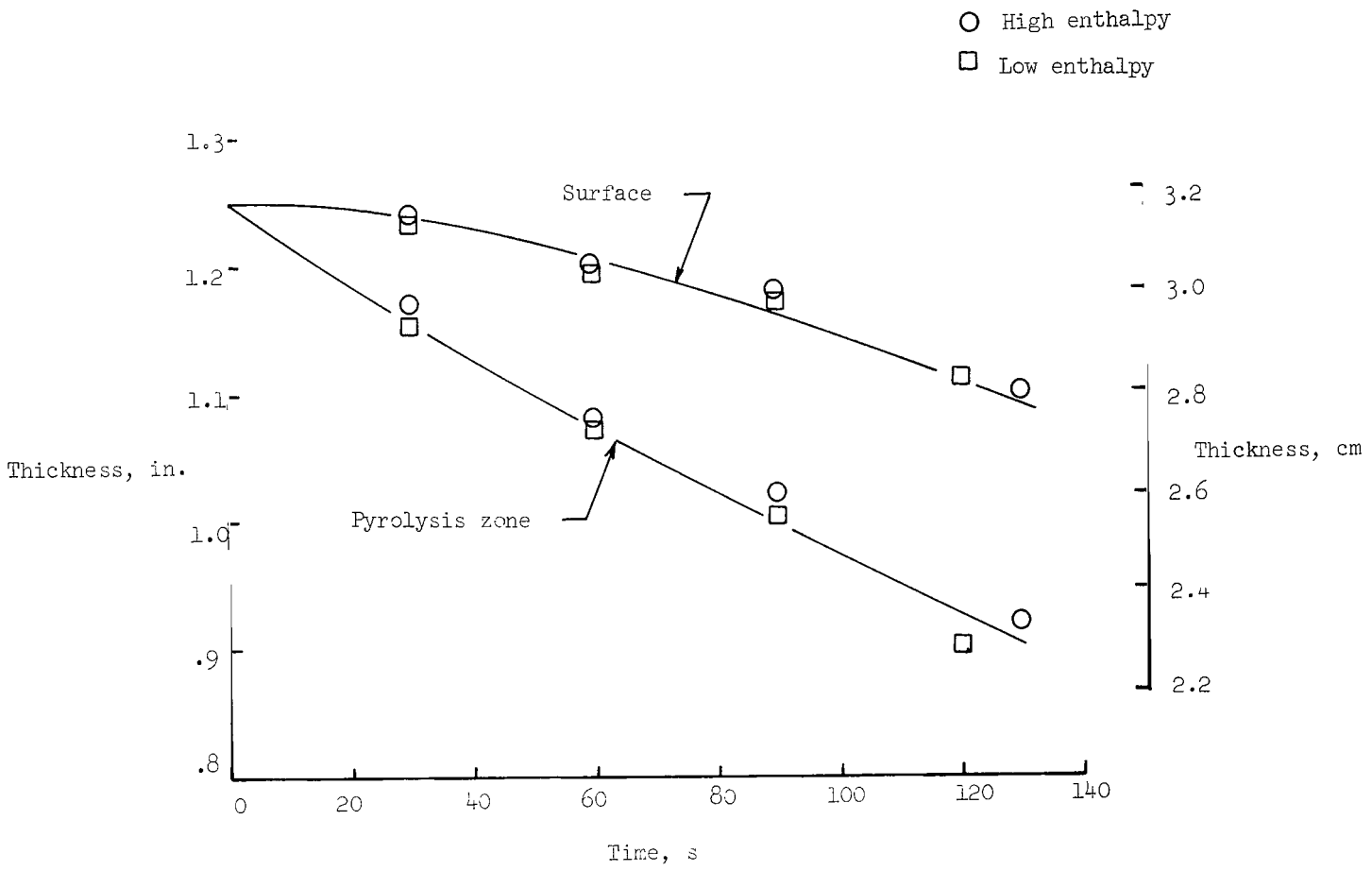

Figure 8.- Measured surface and interface-location histories for high-density phenolic-nylon specimens.

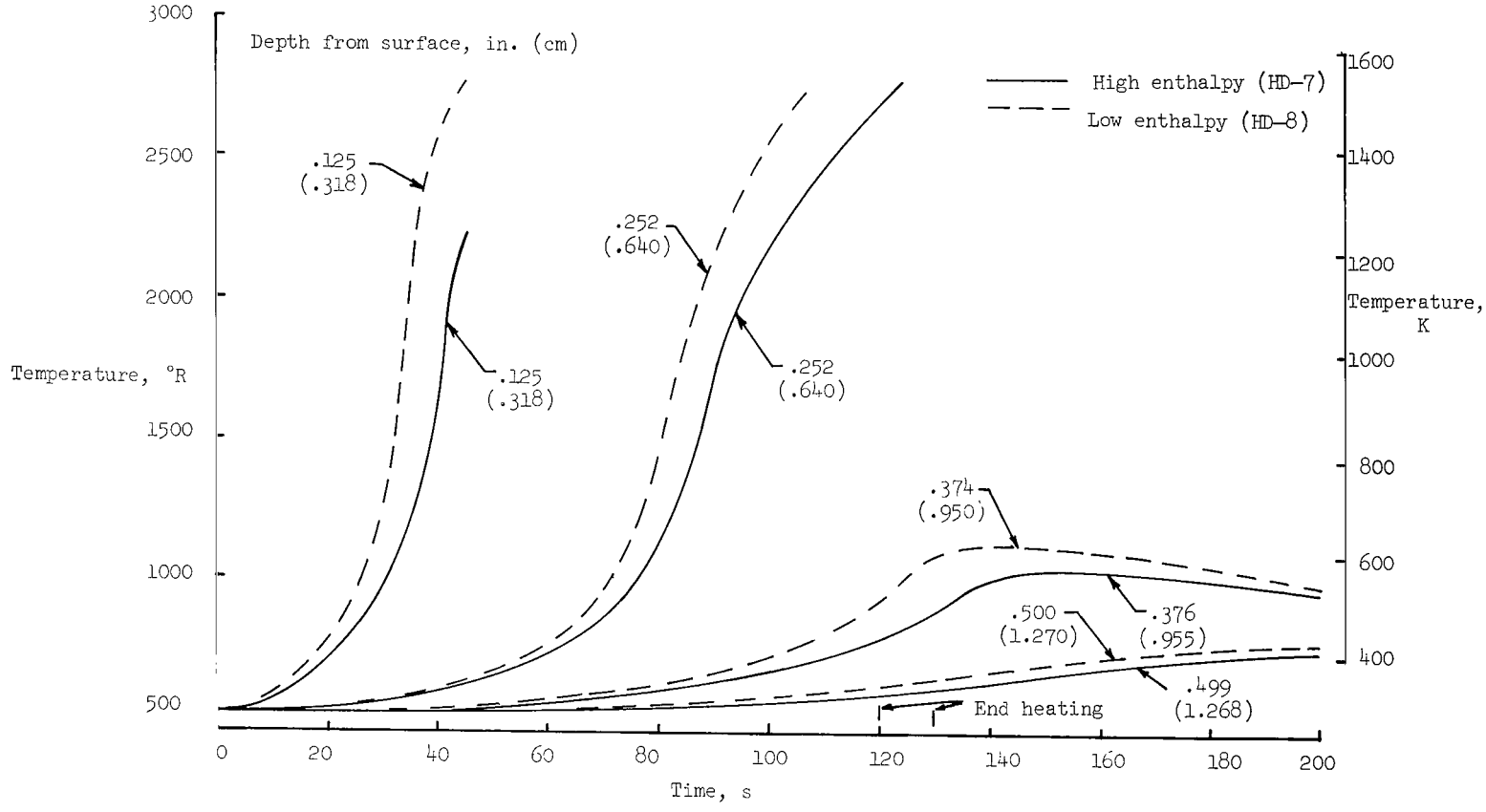

Figure 9.- Measured internal-temperature histories for two high-density phenolic-nylon specimens.

NATIONAL AERONAUTICS AND SPACE ADMINISTRATION
WASHINGTON, D. C. 20546

OFFICIAL BUSINESS

FIRST CLASS MAIL

POSTAGE AND FEES PAID
NATIONAL AERONAUTICS AND
SPACE ADMINISTRATION

"The aeronautical and space activities of the United States shall be conducted so as to contribute . . . to the expansion of human knowledge of phenomena in the atmosphere and space. The Administration shall provide for the widest practicable and appropriate dissemination of information concerning its activities and the results thereof."

—NATIONAL AERONAUTICS AND SPACE ACT OF 1958

NASA SCIENTIFIC AND TECHNICAL PUBLICATIONS

TECHNICAL REPORTS: Scientific and technical information considered important, complete, and a lasting contribution to existing knowledge.

TECHNICAL NOTES: Information less broad in scope but nevertheless of importance as a contribution to existing knowledge.

TECHNICAL MEMORANDUMS: Information receiving limited distribution because of preliminary data, security classification, or other reasons.

CONTRACTOR REPORTS: Scientific and technical information generated under a NASA contract or grant and considered an important contribution to existing knowledge.

TECHNICAL TRANSLATIONS: Information published in a foreign language considered to merit NASA distribution in English.

SPECIAL PUBLICATIONS: Information derived from or of value to NASA activities. Publications include conference proceedings, monographs, data compilations, handbooks, sourcebooks, and special bibliographies.

TECHNOLOGY UTILIZATION PUBLICATIONS: Information on technology used by NASA that may be of particular interest in commercial and other non-aerospace applications. Publications include Tech Briefs, Technology Utilization Reports and Notes, and Technology Surveys.

Details on the availability of these publications may be obtained from:

SCIENTIFIC AND TECHNICAL INFORMATION DIVISION

NATIONAL AERONAUTICS AND SPACE ADMINISTRATION

Washington, D.C. 20546